

Influence of the Reynolds Number on the Open Water Characteristics of Propellers with Short Chord Lengths

H.-J. Heinke, K. Hellwig-Rieck, L. Lübke¹

¹Potsdam Ship Model Basin (SVA), Potsdam, Germany

ABSTRACT

A major engineering task is to obtain the most efficient ship propulsion. For slow steaming ships equipped with low speed engines, propellers with a small blade area have proved to be a promising option to gain efficiency. By reducing the propeller blade area and thus the blade chord length it is intended to reduce the frictional losses and in course of that to improve the propeller performance. If these propellers are investigated in model scale the combination of low rotational speeds and short chord length can lead to very low Reynolds numbers in the propeller open water (POW) tests. In these investigations the Reynolds number can drop below $Re_{c(0.7R)} = 2.0 \cdot 10^5$, which is given as lower Reynolds number limit for POW tests by the ITTC. In this flow conditions the propeller is most likely operating in a laminar flow regime, leading to large Reynolds number effects and difficulties in the extrapolation of the model scale characteristics to full-scale.

In this context the SVA Potsdam applies a procedure to reliably extrapolate the propeller open water (POW) characteristics to full-scale and to conduct consistent propulsion tests, by investigating the propeller at a variety of Reynolds numbers (revolutions). The standard at the SVA Potsdam is to carry out POW tests for at least three rates of revolution. If required the investigations can be extended by additional rates of revolution, until a linear behaviour between the propeller performance coefficients and the Reynolds number is established. This can lead to POW tests up to Reynolds numbers of $Re_{c(0.7R)} = 5.0 \cdot 10^5$. In the course of this paper the procedure applied at the SVA Potsdam is introduced and discussed with respect to the testing and scaling procedure and its application for the propulsion prognosis.

Additionally, numerical simulations of the POW characteristics for different Reynolds numbers under consideration of the laminar-turbulent transition are presented. In these, emphasis is laid upon resolving the flow features occurring at the propeller blade, such as laminar separation and the transition point. Also the capability of CFD to capture the relatively small differences imposed by Reynolds number effects could be demonstrated. In this context different turbulence models

were applied, ranging from the $k\omega$ -SST to the SBES (Stress-blended eddy simulation) turbulence model with γ - Re_{θ} or the intermittency transition model. The CFD calculations were conducted with ANSYS CFX and ANSYS Fluent.

Keywords

Propeller, open water characteristics, Reynolds number, scale effects, laminar-turbulent transition, CFD

1 INTRODUCTION

The demand for low power consumption and high efficiency in the shipping industry has led to a reduction in ship speed (slow steaming) and the application of low speed engines. This allowed the design of propellers with small blade area ratios and short chord length respectively. With this design approach it is intended to reduce the frictional losses of the propeller and gain efficiency. The investigations of these designs is challenging for the testing facilities such as the Potsdam Ship Model Basin (SVA Potsdam), due to the circumstance that the propulsion test have to be conducted at low Reynolds numbers. Since the propulsion tests and the POW tests have to be carried out in equivalent flow conditions, the POW tests have to be carried out at the same rate of revolution and thus at the same Reynolds numbers as the propulsion tests. This can lead to test conditions in which the Reynolds number drops below the recommended limit of the ITTC of $Re_{c(0.7R)} = 2.0 \cdot 10^5$ “(ITTC 2014)“, implying that the propeller operates in laminar flow and that transition effects have to be taken into account. This circumstance leads to a large impact of the Reynolds number on the propeller characteristics, raising questions concerning the propulsion analysis, the Reynolds number correction and the propulsion prognosis. Inconsistencies in the testing procedure can lead to a drop in the relative rotative efficiency η_R .

The Potsdam Model Basin performs the standard propeller open water tests at three different numbers of revolutions (Reynolds numbers) “(Bednarzik 1984)“. Two open water tests are carried out in the Reynolds number range of the model propeller in the propulsion tests. The third open water test is carried out at a higher Reynolds number and is used for the prediction of the full-scale propeller characteristics. The investigations of

propellers with short chord length have shown that the number of POW tests for these propellers has to be increased, in order to obtain reliable propeller performance data. In course of the paper investigations on basis of this background will be presented and discussed.

The issue to cope with the Reynolds number dependency of the POW tests for propellers with short chord length has been addressed by other research groups as well. One approach is to scale the POW characteristics by means of a strip method “(Lücke & Streckwall 2017) “ or to apply a two POW test approach “(Hasuike et al, 2017) “. In both publications it was also demonstrated that laminar-turbulent transition is a major subject for both POW and propulsion tests by means of extensive paint flow tests and numerical calculations.

In the course of this paper the investigations of four model propellers with short chord length are presented. The area ratios of these propellers are ranging from approximately $A_E/A_0 = 0.4$ to 0.6. The model propellers were investigated in the towing tank of the SVA Potsdam in the rotational speed range between 4 to 30 rps, revealing a large impact of the Reynolds number on the POW characteristics. Different scaling procedures were applied and the results of the extrapolation to full-scale are discussed. Furthermore, the effect on the relative rotative efficiency and the propulsion prognoses are demonstrated.

Additionally numerical simulations were conducted with the aim to reproduce the Reynolds number effects for the model scale Reynolds numbers. A major advantage of the CFD methods is the ability to calculate the full-scale propeller, but due to the lack of validation data the investigations are focused on model scale with special attention to the laminar-turbulent transition. In this context different turbulence models are applied, ranging from the $k\omega$ -SST to the SBES (Stress-blended eddy simulation) turbulence model with the γ - Re_θ or the intermittency transition model.

The main goal of all investigations is to improve the reliability of the propulsion prognosis.

2 MODEL PROPELLERS

The propellers for the model tests and the corresponding calculations have been selected from the stock of the SVA. Selection criteria were a small area ratio, a critical Reynolds number range in the propulsion tests and a significant Reynolds number effect at the open water characteristics. In table 1 the main parameters of four model propellers are given, while in table 2 the operation conditions of these propellers in the propulsion tests are shown.

All propellers are fixed pitch propellers with a hub ratio in the range of $d_h/D = 0.151$ to 0.186 and blade area ratios varying between $A_E/A_0 = 0.4$ to 0.6. The chord length on radius $r/R = 0.7$ lies for all propellers between 5 and 7 cm. In Fig.1 the geometry of propeller A is shown exemplarily. Propeller A is mainly used for the CFD calculations.

Table 1: Main parameters of model propellers

Propeller		A	B	C	D
D_M	[m]	0.239	0.239	0.219	0.239
A_E/A_0	[-]	0.418	0.444	0.596	0.498
$c_{0.7M}$	[m]	0.054	0.056	0.057	0.070
Z	[-]	4	4	5	4

Table 2: Operation conditions in propulsion tests

Propeller		A	B	C	D
n_{min}	[s ⁻¹]	4.79	4.75	5.08	6.03
Re_{min}	[10 ⁵]	1.25	1.29	1.38	2.14
n_{max}	[s ⁻¹]	7.29	7.19	9.11	9.98
Re_{max}	[10 ⁵]	1.89	1.95	2.47	3.54

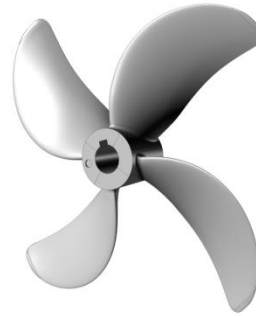


Fig. 1: Propeller A

3 OPEN WATER TESTS

The POW tests have been carried out in the towing tank of the SVA Potsdam using the propeller dynamometers H29 ($Q_{max} = 15$ Nm, $T_{max} = 400$ N) and H39 ($Q_{max} = 55$ Nm, $T_{max} = 1000$ N). In Fig. 2 this type of dynamometer is shown, with H29 and H39 having a specific performance profile. Each POW curve is obtained for a given rotational speed via a variation in advance speed. The Reynolds number variation is achieved by applying different rotational speeds.

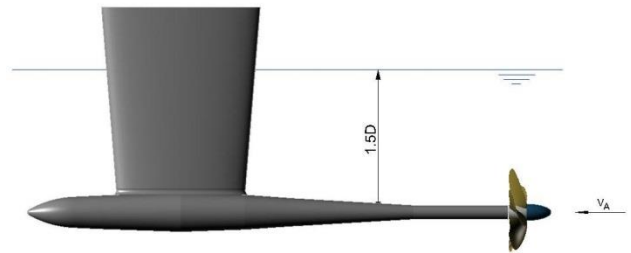


Fig. 2: Open water propeller dynamometer

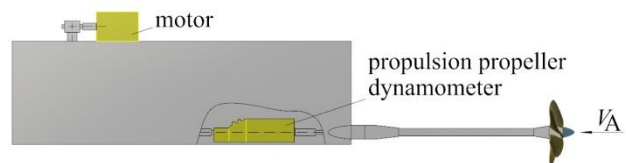


Fig. 3: Open water box with propulsion propeller dynamometer

The standard propeller dynamometers can measure large forces and are designed for high rotational speeds. However, the measuring accuracy for low rotational speeds/forces, as necessary for the operating points given in Tab. 2, is too low. For this reason a special open water box shown in Fig. 3 was introduced, having the advantage that the dynamometer can be replaced to meet the specific demands for the tests. For example the dynamometer R31 ($Q_{\max} = 4 \text{ Nm}$, $T_{\max} = 100 \text{ N}$), intended for propulsion tests with ship models, can be arranged in the box, making it possible to choose always the most suitable dynamometer for the specific application and to obtain accurate measurements.

4 MEASURED OPEN WATER CHARACTERISTICS

POW tests have been carried out at rotational speeds of $n_M = 5, 8, 10, 18, 22$ and 26 s^{-1} . The used dynamometers have been adapted to the specific measuring range.

The open water characteristics measured at the rotational speeds of $n_M = 5, 8$ and 10 s^{-1} were required for the analysis of the propulsion tests (determination of the thrust wake fraction w_T and the relative rotative efficiency η_R), while $n_M = 18, 22$ or 26 s^{-1} were used for the extrapolation to the full-scale propeller characteristics.

In Fig. 4 the measured open water characteristics of propeller A are shown. The POW curves were obtained by multiple repetitions of the measurements. The corresponding Reynolds numbers were determined at the blade radius $0.7 R$, according to equation (1).

$$Re_{c(0.7R)} = \frac{c_{0.7}}{\nu} \cdot \sqrt{V^2 + (0.7 \cdot D \cdot \pi \cdot n)^2} \quad (1)$$

The variation in Reynolds number between $Re_{c(0.7R)} = 1.4 \cdot 10^5$ to $6.9 \cdot 10^5$ showed a strong impact on the POW characteristics.

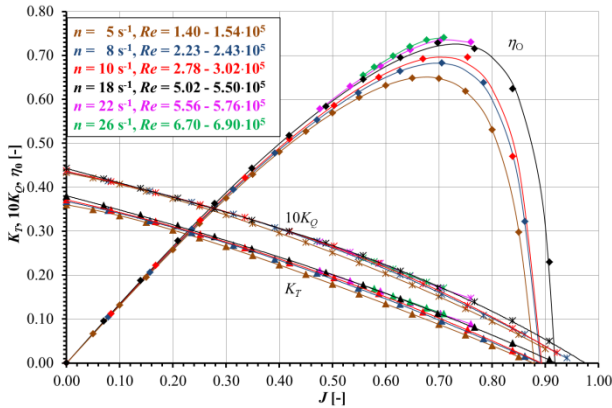


Fig. 4: Open water characteristics of propeller A

The analysis of the open water characteristics of all four propellers shows the following tendencies:

- Thrust and torque coefficients, measured in the rotational speed range $n_M = 5 - 20 \text{ s}^{-1}$ are mainly increasing with the Reynolds number.
- The increase of the propeller efficiency with rising Reynolds number in the rotational speed range of $n_M = 5 - 20 \text{ s}^{-1}$ is mainly caused by the increase in thrust coefficient.

- At Reynolds numbers $Re_{c(0.7R)} > 5.0 \cdot 10^5$ the thrust coefficients are nearly constant, while the torque coefficient decreases linearly with rising Reynolds number.

In Fig. 5 the thrust and torque coefficients and the open water efficiency for propeller A are plotted over the investigated Reynolds number range for advance coefficient $J = 0.55$ (design point). The variation in propeller coefficients for propeller B at $J = 0.56$ is shown in Fig. 6.

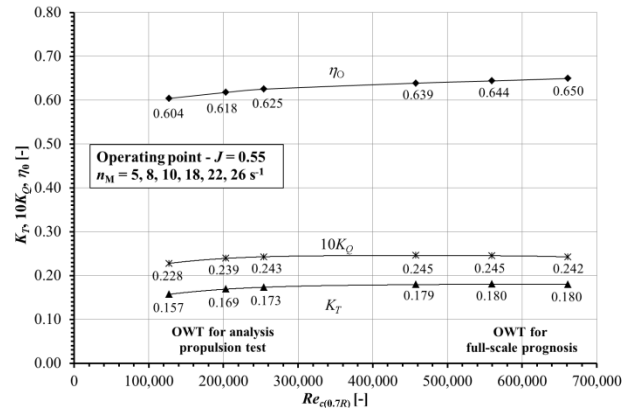


Fig. 5: Variation of propeller coefficients of propeller A with the Reynolds number

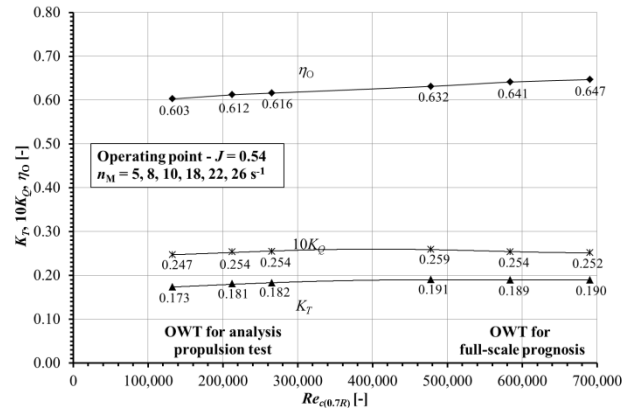


Fig. 6: Variation of propeller coefficients of propeller B with the Reynolds number

The behavior of the thrust and torque at the lower Reynolds numbers stands in contradiction to the general expectations of the Reynolds number effects with decreasing torque and almost constant thrust coefficients.

5 CALCULATED OPEN WATER CHARACTERISTICS

The spread in POW characteristics for the propellers with short chord length within the relatively small Reynolds number range of the model tests has raised questions concerning the flow around the propellers. Numerical calculations were conducted with the goal to reproduce these Reynolds number effects in the simulations.

In general two approaches in CFD are apparent. One is to concentrate on full-scale “(Bulten & Stoltenkamp, 2017)”, while the other remains in model scale and evaluates the results with experimental data. These approaches do not need to be mutually exclusive, but can

be practised alternately. In the course of this paper the numerical simulations are confined to model scale.

5.1 Numerical Model

The numerical simulation of the laminar-turbulent transition requires carefully generated numerical meshes. For the dimensionless wall distance values smaller than 1 ($y^+ < 1$) are a must. Furthermore the mesh expansion factors in the boundary layer should not exceed 1.2 but should be kept around 1.1. From the authors experience also the mesh resolution in stream wise direction is a decisive factor. Although no precise recommendations can be given, the cell number in stream wise direction should be large, also to limit the cell aspect ratios in the boundary layer. The recommendations for the grid generation have to be observed in order to obtain accurate results.

For the numerical modeling of the transitional flow different models were employed. Steady simulations with ANSYS CFX, the $k\omega$ -SST turbulence model, the γ - Re_θ transition model and the coupled solver were carried out. The two equation transition model solves for the intermittency and the transition onset Reynolds number. Furthermore the SBES (Stress Blended Eddy Simulation) turbulence model with the intermittency transition model was employed in unsteady simulations with ANSYS Fluent and the segregated solver. The SBES simulations were conducted to obtain a more profound insight into the flow details. The one equation transition model solves only the turbulence intermittency equation and avoids the need for the Re_θ equation. The intermittency model can account for crossflow instability, which might be relevant for flows with higher turbulence intensity ($T_u > 1\%$). However, the flow in the towing tank is of smaller turbulence intensity.

The selected numerical schemes were of second order, with the bounded central differencing scheme employed in conjunction with the SBES turbulence model.

The CFX simulations were carried out with unstructured tetrahedral meshes. For the Fluent simulations the unstructured mesh was converted to a polyhedral mesh with preservation of the prism-layer on the blade and hub. The simulations were carried out for a single blade passage with periodic boundaries. Altogether the numerical meshes had cell numbers between 6 (steady, $k\omega$ -SST) and 12 Million cells (SBES). In Fig.7 the numerical mesh on the blade and the periodic boundary for the Fluent simulations are given.

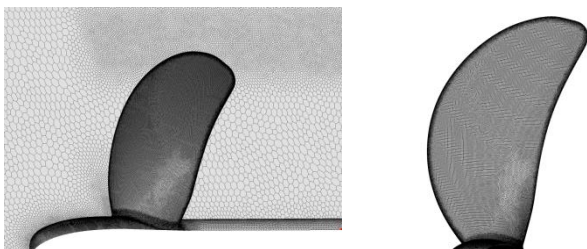


Fig. 7: Numerical mesh

The laminar-turbulent transition is sensitive to the turbulence intensity “(Langtry & Menter, 2005) “. However, a major drawback in the simulations is the rapid decay of the turbulence intensity given at the inlet. For the numerical simulations a variation of turbulence intensity at the inlet was carried out, in order to obtain the desired turbulence level at the propeller. The CFD calculations are validated with POW curves measured in the towing tank of the SVA Potsdam. The turbulence intensity in the towing tank is considered to be low.

5.2 Flow Characteristic

In the evaluation of the numerical simulations special attention was laid upon the laminar separation and the transition zone. The visualization of the flow was carried out for the SBES calculations only.

In Fig. 8 the limiting streamlines and the vortex core region for the Lambda2 criterion of 0.01 are shown on the suction (left) and pressure (right) side for propeller A. The simulations were conducted for the turbulence intensity of $T_u = 0.2\%$. The flow is predominantly laminar, as indicated by the radial progression of the streamlines on the blade. On the suction side of the propeller the flow is separating, as the adverse pressure gradients near the trailing edge of the blade gets too high. However, this does not automatically mean, that transition to turbulent flow occurs. The flow winds up and shows curly flow structures which are not necessarily turbulent.

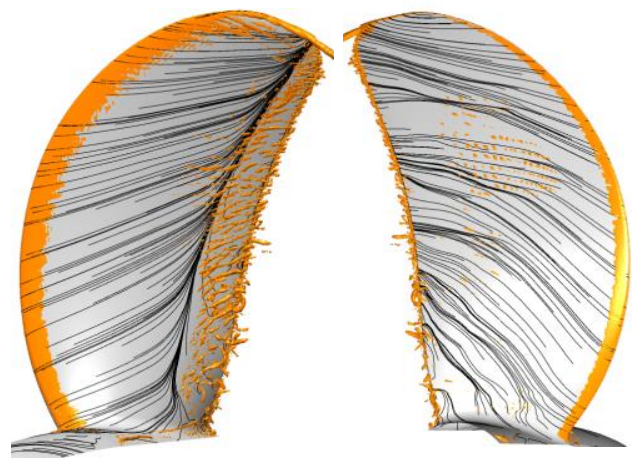


Fig. 8: Limiting streamlines and vortex core region for propeller A ($J = 0.55$ and $n_M = 10 \text{ s}^{-1}$) for the turbulence intensities of $T_u = 0.2\%$ for the suction (left) and pressure (right) side

On the pressure side of the propeller blades laminar turbulent transition occurs on the higher radii in the forward quarter of the blade sections. The transition of the flow is initiated by instabilities in the flow forming turbulent stripes, which eventually cause the flow to become fully turbulent. This is also shown in Fig. 9, giving the distribution of the turbulent kinetic energy k in different planes intersecting the propeller blade.

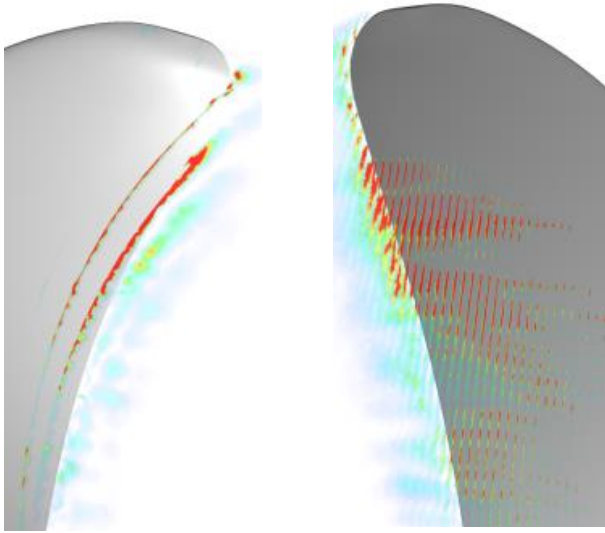


Fig. 9: Turbulent kinetic energy on the blade of propeller A for $J = 0.55$, $n = 10 \text{ s}^{-1}$ and $T_u = 0.2 \%$

The propeller forces and moments are dominated by the pressure component, with only a small contribution by the frictional forces. This applies of course also for laminar flow. It shows that in case this propeller operates in a laminar flow regime also a decisive scale effect on the thrust can be observed.

With respect to transition, the propeller characteristics are influenced by a variety of factors, making the simulation of these conditions rather difficult. The transition point can differ between suction and pressure side. Also, the flow separates more easily, in case of adverse pressure gradients. These two phenomena are again influenced by the Reynolds number and the turbulence intensity in the flow. Geometrical parameters, as for example leading edge radius or thickness distribution of the foil sections, might also have an impact on the propeller characteristics.

The applied computations are able to give an insight in the flow phenomena occurring in laminar-turbulent transition and make it possible to address also Reynolds number effects in the simulations.

5.3 Reynolds Number Effects

The thrust and torque coefficient and the open water efficiency were calculated for the advance coefficient $J = 0.56$ for different Reynolds numbers. In the CFD calculations one additional operating point was investigated ($n_M = 36 \text{ s}^{-1}$). The computational results were compared to the corresponding POW test results, as shown in Fig. 10. The computational results were obtained with the $k\omega$ -SST turbulence and the γ - Re_θ transition model. It shows that in general a good agreement between computations and measurements is obtained. For the rotational speeds of $n_M = 8$ and 10 s^{-1} however, the deviation between the computational and the experimental results is slightly larger. The reason is thought to be a non-optimal value for the dimensionless wall distance.

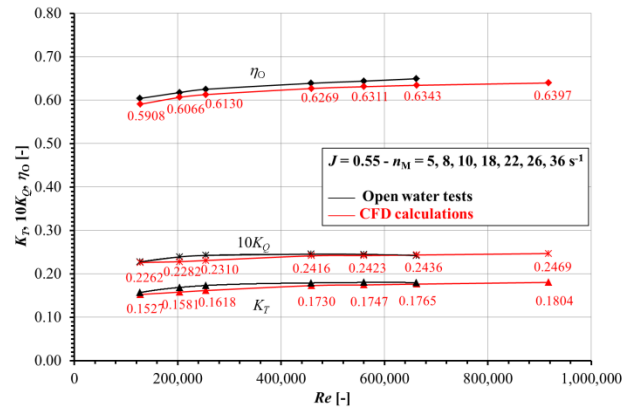


Fig. 10: Variation of propeller coefficients of propeller A with the Reynolds number - comparison of calculated and measured values

In total the numerical simulations seem to capture the Reynolds number effects, occurring at the propeller in the investigated Reynolds number range, rather good. For low Reynolds numbers also the thrust is affected by scale-effects. The propeller A shows the expected behavior only above the Reynolds number of $Re_{c(0.7R)} = 5.0 \cdot 10^5$.

6 REYNOLDS NUMBER CORRECTION

Due to the inability to obtain Reynolds number similarity in open water tests, the propeller characteristics have to be corrected to full-scale. The Reynolds number correction procedure 1978 ITTC Performance Prediction Method “(ITTC 2014)”, the method of Lerbs/Schmidt “(Lerbs 1951, Schmidt 1972)” and the method of SVA “(Schulze 2017, Klose 2017)” have been used for the prediction of the full-scale open water characteristic of the propellers.

The 1978 ITTC Performance Prediction Method is the standard procedure for the correction of scale effects on the propeller characteristics. The method of Lerbs/Schmidt applies foil theory and tries to determine the Reynolds number effects on basis of an “equivalent airfoil section”. The open water coefficients K_T and K_Q are converted to the foil coefficients C_L and C_D in dependency of the angle of attack. The Reynolds number correction procedure developed by SVA follows mainly the basic principles of the 1978 ITTC Performance Prediction Method. Modifications were applied for the calculation of the friction resistance. The three procedures refer to the propeller radius $r/R = 0.75$ only.

The different Reynolds number correction procedures have been applied to the open water characteristics of the propellers, with the influence being exemplarily demonstrated for propeller A. In Fig. 11 the uncorrected open water curves are given for a limited set of rotational speeds ($n_M = 5, 8, 10$ and 18 s^{-1}). The values for the rotational speed of $n_M = 5 \text{ s}^{-1}$ are below the recommended Reynolds number limit of $Re_{c(0.7R)} = 2.0 \cdot 10^5$. For the full-set of investigated rotational speeds refer to Fig. 4.

The 1978 ITTC Performance Prediction Method transfers the measured differences in the POW characteristics to full-scale, as shown in Fig. 12. The open water efficiency

varies with the selection of the POW curves, making the full-scale prediction uncertain.

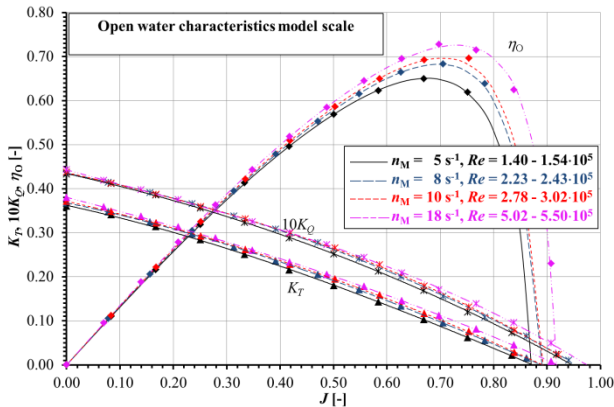


Fig. 11: Open water characteristics of propeller A used for the Reynolds number correction

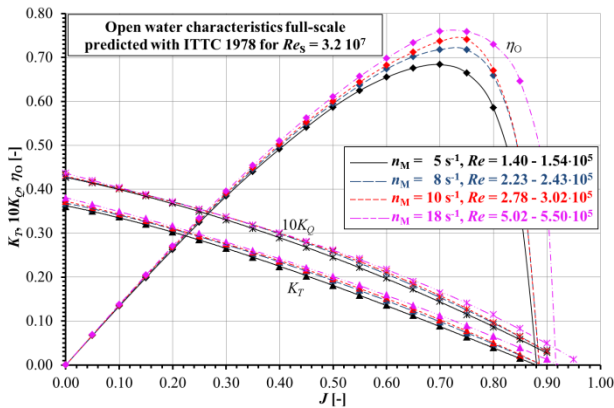


Fig. 12: Open water characteristics of propeller A predicted with 1978 ITTC Performance Prediction Method for $Re_{c(0.7R)} = 3.2 \cdot 10^7$

The Reynolds number correction method of Lerbs/Schmidt cannot be used for open water characteristics measured below $Re_{c(0.7R)} = 2.0 \cdot 10^5$. For higher Reynolds numbers the method of Lerbs/Schmidt predicts in the region of interest the same full-scale open water efficiency independent of the Reynolds number of the model test, as shown in Fig. 13.

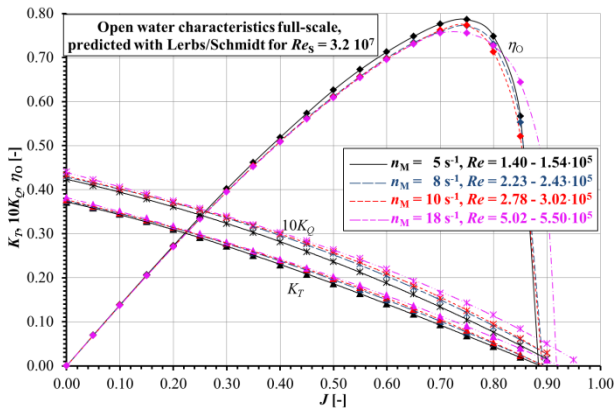


Fig. 13: Open water characteristics of propeller A predicted with Method of Lerbs/Schmidt for $Re_{c(0.7R)} = 3.2 \cdot 10^7$

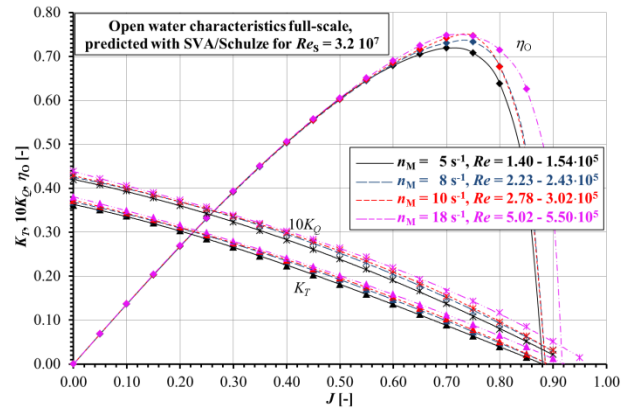


Fig. 14: Open water characteristics of propeller A predicted with Method of SVA/Schulze for $Re_{c(0.7R)} = 3.2 \cdot 10^7$

For the method of SVA/Schulze it can also be observed that around the design point the same open water efficiency is obtained in full-scale, regardless of the model scale rotation rate/Reynolds number used for the extrapolation. In Fig. 14 the extrapolated open water characteristics predicted with the method of SVA/Schulze are shown.

The extrapolation methods of Lerbs/Schmidt and SVA/Schulze show that they can account for laminar or partially laminar flow conditions in the propeller flow. The 1978 ITTC Performance Prediction Method fails to give reliable full-scale POW curves, for laminar or partially laminar flow conditions. Therefore, it is necessary for propellers with short chord length to conduct POW tests also at higher Reynolds numbers. For the investigated propellers the Reynolds number had to be pushed up to values of $Re_{c(0.7R)} > 5.0 \cdot 10^5$, in order to make the ITTC method applicable.

As an indicator whether the Reynolds number is high enough for a full-scale extrapolation by the 1978 ITTC Performance Prediction Method, the trend in the thrust and torque coefficients has to be analysed. The thrust has to be nearly constant and the torque has to be gradually decreasing, as shown in Fig. 5 and 6 for sufficiently high Reynolds numbers. Following this approach at least two POW test have to be conducted for the full-scale Reynolds number, enabling to derive the trend between the two Reynolds numbers.

In case the 1978 ITTC Performance Prediction Method is applied on basis of POW curves with sufficiently high Reynolds numbers, all three extrapolation methods give similar results, as shown in Fig. 15. The SVA/Schulze method predicts the full-scale POW efficiency slightly lower than the other two methods.

With the method of Lerbs/Schmidt the extrapolation to full-scale would also work on basis of the POW curves with lower rotational speeds ($n_M = 8$ and 10 s^{-1}), however it is not an established procedure and therefore not commonly applied.

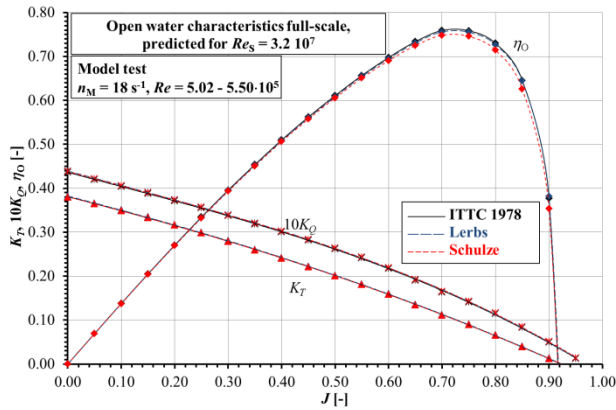


Fig. 15: Open water characteristics of propeller A predicted with different methods for $Re_{c(0.7R)} = 3.2 \cdot 10^7$ using the OWT at $Re_M > 5.0 \cdot 10^5$

7 PROPULSION PROGNOSIS

The analysis of the POW tests in the towing tank show that the model propeller operates in the transition zone between laminar and turbulent flow. This is the reason why the variation in rotational speed (Reynolds number) has such a large impact on the propeller coefficients. Open water tests with a sufficiently high Reynolds number ($Re_{c(0.7R)} > 5.0 \cdot 10^5$) should be used for the prognosis of the open water characteristics of the full-scale propeller.

At least two open water tests should be carried out in the rotational speed range of the propeller in the propulsion tests. By means of interpolating between the open water characteristics the corresponding coefficients for each required point in the propulsion prognoses can be derived. In this way a high precision in the determination of the propulsion coefficients, thrust wake fraction w_T and relative rotative efficiency η_R can be achieved in the investigated speed range of the ship model.

The SVA has established a three to five point POW test method for the determination of the propulsion coefficients and for the calculation of the full-scale open water characteristics. Using this method the thrust wake fractions w_T and the relative rotative efficiencies η_R are nearly constant for the tested ship speed range (Table 3).

Table 3: Example of propulsion prognosis with 4 POW tests

V	t	w_T	η_R	η_D	η_o
[kn]	[-]	[-]	[-]	[-]	[-]
10.00	0.182	0.289	1.018	0.798	0.682
11.00	0.180	0.287	1.017	0.798	0.683
12.00	0.183	0.287	1.017	0.795	0.682
13.00	0.190	0.290	1.017	0.788	0.680
14.00	0.198	0.292	1.018	0.780	0.677
15.00	0.198	0.290	1.016	0.773	0.674

8 SUMMARY

A thorough analysis of the POW characteristics for propellers with short chord length in model scale is presented. It is shown, that propellers with short chord length have to be investigated under consideration of the laminar-turbulent transition, occurring in case of low rotation rates. This makes it necessary to carry out multiple POW tests. The SVA Potsdam has developed a procedure with three to five POW tests, in order to secure the propulsion prognosis. In this way inconsistencies in the propulsion prognosis regarding e.g. the relative rotative efficiency can be avoided and the quality of the prognosis can be secured. To obtain reliable results it is considered necessary to conduct POW tests up to Reynolds numbers of $Re_{c(0.7R)} > 5.0 \cdot 10^5$. To also secure accurate POW test measurements for very low Reynolds numbers an open water box has been introduced, making it possible to select the most suitable dynamometer for the task.

The experimental investigations were supplemented by numerical simulations. The CFD simulations were conducted to verify whether it is possible to capture the relatively small Reynolds number effects in the investigated model scale Reynolds number range. The evaluations of the results show that a good agreement between computational and experimental results is achieved and that for example the impact of the Reynolds number on the thrust coefficient can be reproduced. Due to laminar flow it can occur that the thrust coefficient decreases for the same advance coefficient with decreasing Reynolds number. Only with a sufficiently high Reynolds number the thrust coefficient reaches a kind of plateau and remains almost constant. For the extrapolation to full-scale it is necessary to secure that the propeller characteristics have reached this point and show a linear behavior with increasing Reynolds number.

Furthermore CFD simulations have been conducted to obtain a better insight in the flow phenomena occurring during the laminar-turbulent transition. The investigations have shown that turbulent stripes being generated at the blade surface trigger the transition process. In all investigations laminar separation could be observed at the trailing edge of the suction side.

ACKNOWLEDGEMENT

The authors would like to express their gratitude to the Federal Ministry for Economic Affairs and Energy for funding the research project.

NOMENCLATURE

CFD	computational fluid dynamics
POW	propeller open water (e.g. test)
SST	Shear Stress Transport
SBES	Strain Blended Eddy Simulation

A_E/A_0	[-]	expanded blade area ratio
C_F	[-]	friction coefficient
C_D	[-]	drag coefficient
C_L	[-]	lift coefficient
c	[m]	chord length
D	[m]	propeller diameter
J	[-]	advance coefficient $V_A / (D n)$
k	[m ² /s ²]	turbulence kinetic energy
n	[1/s]	number of revolutions
Q	[Nm]	torque
K_Q	[-]	torque coefficient $Q / (\rho n^2 D^5)$
K_T	[-]	thrust coefficient $T / (\rho n^2 D^4)$
k_p	[m]	blade roughness 10E-6 m
k_{tech}^+	[-]	technical roughness
P	[m]	propeller pitch
p	[Pa]	pressure
r	[m]	local radius
R	[m]	propeller radius
Re	[-]	Reynolds number VL / ν
T	[N]	propeller thrust
T_u	[%]	turbulent intensity
t	[m]	blade thickness
V_A	[m/s]	inflow velocity
Z	[-]	blade number
α	[°]	angle of attack
η_0	[-]	open water efficiency
ρ	[kg/m ³]	density of fluid

REFERENCES

- Bednarzik, R. (1984). 'Zur Berücksichtigung des Reynoldszahl- und Rauigkeitseinflusses auf die Propellerfreifahrtcharakteristiken', Schiffbauforschung 3.
- Lücke, T., Streckwall, H. (2017) 'Experience with Small Blade Area Propeller Performance', Fifth International

- Symposium on Marine Propulsors, SMP'17, Espoo, Finland
- Hasuike, N., Okazaki, M., Okazaki, A., Fujiyama, K. (2017). 'Scale effects of marine propellers in POT and self-propulsion test conditions'. Fifth International Symposium on Marine Propulsors, SMP'17, Espoo, Finland
- Bulten, N., Stoltenkamp, P. (2017). 'Full-scale CFD: The end of the Froude-Reynolds battle'. Fifth International Symposium on Marine Propulsors, SMP'17, Espoo, Finland
- Menter, F., Langtry, R. (2005). 'Overview of Transition Model Test Cases'. ANSYS Report, 2005
- Müller, S.-B., Abdel-Maksoud, M., Hilbert, G. (2009). 'Scale effects on propellers for large container vessels'. First International Symposium on Marine Propulsors, SMP'09, Trondheim, Norway
- Wang, X., Walters, K. (2012). 'Computational Analysis of Marine-Propeller Performance Using Transition-Sensitive Turbulence Modeling'. Journal of Fluids Engineering, July 2012, Vol. 134 / 071107-1
- ITTC (2014). '1978 ITTC Performance Prediction Method'. Recommended Procedures and Guidelines 7.5-02-03-01.4.
- Lerbs, H. W. (1951). 'On the Effects of Scale and Roughness on Free Running Propellers'. J.A.S.N.E., Report 63.
- Schmidt, D. (1972). 'Einfluss der Reynoldszahl und der Rauigkeit auf die Propellercharakteristik, berechnet nach der Methode des äquivalenten Profils'. Schiffbauforschung 11.
- Klose, R., Schulze, R., Hellwig-Rieck, K. (2017). 'Investigation of Prediction Methods for Tip Rake Propellers', Fifth International Symposium on Marine Propulsors, SMP'17, Espoo, Finland.
- Schulze, R. (2017). 'A new friction correction method for the open water characteristics of propellers'. STG Annual Book, Hamburg.